International Journal of Pure and Applied Mathematics
Volume 100 No. 2 2015, 193-209
ISSN: 1311-8080 (printed version); ISSN: 1314-3395 (on-line version)
url: http://www.ijpam.eu
doi: http://dx.doi.org/10.12732/ijpam.v100i2.3

TRANSIENT SPECTRUM OF $\sin^2$-PULSED-DRIVEN QUBIT

R.A. Alharbey

Department of Mathematics
Faculty of Science
King AbdulAziz University
Jeddah, KINGDOM OF SAUDI ARABIA

Abstract: The model of a non-dissipative qubit (taken as a single 2-level atom) coupled to a short resonant laser pulse of $\sin^2$-shape is investigated through the transient fluorescent spectrum. Exact analytical operator solutions for the model Heisenberg equations are utilised to calculate the spectrum in terms of Bessel functions. Asymmetry and ringing in the 3-peak spectrum with strong Rabi frequency are pronounced with initial atomic coherent state as compared with the ground state case. This is due to interference of the sequential-pulse structure of the $\sin^2$-pulse with the initial dispersive coherence. For moderate Rabi frequency, ringing disappears with ' hole burning' dip shown in the dominant central Lorentzian peak.

Key Words: driven qubit, $\sin^2$-pulse, scattered spectrum

1. Introduction

The subject of investigating the nature of the emitted radiation due to the interaction of an atomic system with laser field is known as resonance fluorescence (RF). The simplest model is the dissipative single 2-level atom interacting with an idealised mono-chromatic laser field [1]. In the case of strong laser field,

Received: August 12, 2014

the emitted (fluorescent) spectrum shows a triplet Lorentzian structure (Stark triplet) cantered at frequencies: $\omega_l, \omega_l \pm \Omega$ with ω_l is the laser circular frequency, Ω is the Rabi frequency associated with the laser field strength, which has been confirmed experimentally by many researchers [2]-[4]. On the other hand and of equal interest is the investigation of non-dissipative atomic systems driven by short laser pulses of various shapes [5, 6]. In addition to its fundamental interest, pulsed lasers are used to manipulate radiation processes in matter-radiation interaction, to achieve atomic coherent state, which is essential in quantum computation and quantum information processing [7, 8]. Also, important application of short laser pulses exciting non-dissipative atomic system are: the generation of small-sized materials [9] , producing of ultra fast spectroscopic devices [10] and atomic coherent population transfer [11]-[13]

Different shapes of pulsed lasers (rectangular, hyperbolic-secant, Gaussian, triangular, exponential, etc.) have been theoretically examined in the literature, e.g. [5,14-22]. The aim of the present paper is to calculate analytically the transient fluorescent spectrum of a qubit (taken as a non-dissipative 2-level atom) and driven by a resonant $\sin^2$-laser pulse and computationally present the results and its physical interpretation for various system preparations. The $\sin^2$-laser pulse is composed of n-sequential pulses over the period $[0, n\pi]; n \geq 1$ and each pulse of duration π.

The paper is presented as follows. In Sec.2, we present the model Hamiltonian and the explicit exact operator solutions for the atomic variables in the case of exciting resonant laser pulse of $\sin^2$-shape. The dynamics of the mean atomic inversion and polarisation are investigated for initial ground and atomic coherent states. In Sec.3, we calculate the transient spectrum for both initial ground and atomic coherent states with computational investigations. A summary is given in Sec.4.

2. Heisenberg Equations and Solutions

The total Hamiltonian operator modelling the interaction of a single two-level atom of excited and ground states $|e\rangle$ and $|g\rangle$, respectively, with a transition frequency ω_o and laser pulse of circular (envelope) frequency ω_l within electric dipole and rotating wave approximations (in units of $\hbar = 1$, where $\hbar$ is Planck's constant) has the form (cf. [19])

$$\hat{H} = \omega_o \hat{S}_z(t) + \frac{\Omega(t)}{2}(e^{-i\omega_l t}\hat{S}_+(t) + h.c.). \tag{1}$$

Here the real parameter $\Omega(t) = \Omega f(t)$, Ω is the associated laser Rabi frequency, the dimensionless parameter $f(t)$ represents the pulse shape and h.c. stands for hermitian conjugate. In the case of $\sin^2$- laser pulse we have,

$$f(t) = sin^2(n\omega_o t); \quad n = 1, 2, .. \tag{2}$$

where $(n\omega_o)$ is the beating frequency, clearly, the pulse-shape in (2) represents n-sequential pulses, each of time duration (π) over the interval $[0, n\pi]$-(see Fig.1, for the case of $n = 5$).

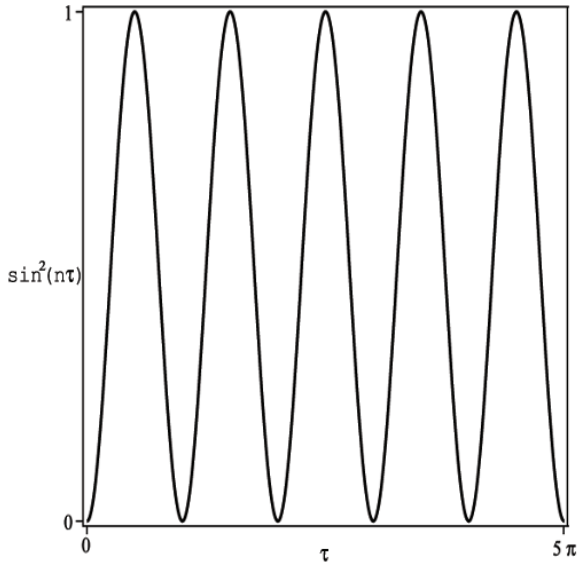

Fig.1: Plot of $f(\tau) = \sin^2(n\tau)$ against normalised time $\tau = \omega_o t$ for $n = 5$

The spin-$\frac{1}{2}$ atomic operators in (1), $\hat{S}_+, \hat{S}_- = (\hat{S}_+)^\dagger$ and $\hat{S}_z$ obey the commutation relations

$$\left[\hat{S}_\pm, \hat{S}_z\right] = \mp\hat{S}_\pm, \left[\hat{S}_+, \hat{S}_-\right] = 2\hat{S}_z, \tag{3a}$$

with further algebraic properties,

$$\hat{S}_\pm^2 = 0, \ \hat{S}_z^2 = \frac{1}{4}. \tag{3b}$$

In the resonance case $(\omega_l = \omega_o)$ and upon introducing the rotating operators,

$$\hat{\sigma}_{\pm}(t) = \hat{S}_{\pm}(t)e^{\pm i\omega_o t} \tag{4a}$$

and denote,

$$\hat{\sigma}_z(t) \equiv \hat{S}_z(t) \tag{4b}$$

with $\hat{\sigma}_{\pm,z}(t)$ obey the same form of commutation and algebraic relations in (3) and according to the Hamiltonian, Eq.(1), Heisenberg equations for the operators $\hat{\sigma}_{\pm,z}(t)$ are of the form,

$$\begin{aligned}\dot{\hat{\sigma}_+} &= -i\Omega(t)\hat{\sigma}_z \\ &= (\dot{\hat{\sigma}_-})^\dagger \\ \dot{\hat{\sigma}_z} &= -i\frac{\Omega(t)}{2}\left(\hat{\sigma}_+ - \hat{\sigma}_-\right)\end{aligned} \tag{5}$$

The exact operator solutions of (5) for arbitrary pulse shape are given by [19],

$$\begin{aligned}\hat{\sigma}_+(t) &= C_+(t)\hat{\sigma}_+(0) + C_-(t)\hat{\sigma}_-(0) + C_z(t)\hat{\sigma}_z(0) = (\hat{\sigma}_-(t))^\dagger \\ \hat{\sigma}_z(t) &= \hat{\sigma}_z(0)\cos\omega(t) - \frac{i}{2}\left(\hat{\sigma}_+(0) - \hat{\sigma}_-(0)\right)\sin\omega(t)\end{aligned} \tag{6}$$

where, the c-number functions $C_{\pm,z}(t)$ are given by,

$$\begin{aligned}C_\pm(t) &= \frac{1}{2}(1 \pm cos\,\omega(t)), \\ C_z(t) &= -isin\,\omega(t)\end{aligned} \tag{7}$$

with,

$$\omega(t) = \Omega \int_0^t f(t')dt'.$$

In the case of $\sin^2$-laser pulse, (2), the time dependent normalised parameter $\omega(t) \to \omega_n(t)$ and its is given by,

$$\omega_n(t) = \frac{\Omega}{2}\left(t - \frac{1}{2n\omega_o}\sin(2n\omega_o t)\right) \tag{8a}$$

or,

$$\omega_n(\tau) = \frac{\Omega'}{2}\left(\tau - \frac{1}{2n}\sin(2n\tau)\right) \tag{8b}$$

where the last form (8b) is written in terms of normalised parameters ($\tau = \omega_o t\, and\, \Omega' = \frac{\Omega}{\omega_o}$).

We now consider the following cases of initial atomic states:

(i) *Initial ground state* $|g\rangle$

In this case the mean atomic variables at $t = 0$ are given by,

$$\langle\hat{\sigma}_{\pm}(0)\rangle_g = 0, \langle\hat{\sigma}_z(0)\rangle_g = -\frac{1}{2} \tag{9}$$

and hence the time-dependent atomic average of (6) simply gives,

$$\langle\hat{\sigma}_{+}(\tau)\rangle_g = \frac{1}{2} i \sin(\omega_n(\tau)),$$
$$\langle\hat{\sigma}_z(\tau)\rangle_g = -\frac{1}{2}\cos(\omega_n(\tau)). \tag{10}$$

As expected with initial ground state, the dispersive component of the atomic polarisation, $Re(\langle\hat{\sigma}_{+}(\tau)\rangle_g) = 0$ at exact resonance, while the absorptive component $Im(\langle\hat{\sigma}_{+}(\tau)\rangle_g) \neq 0$. For $\Omega' = 10^{-3}, n = 1$ the transient behaviour of the mean absorptive polarisation component $Im\langle\hat{\sigma}_{+}(\tau)\rangle_g$ and atomic inversion $\langle\hat{\sigma}_z(\tau)\rangle_g$ are shown in Fig.(2a,b), respectively.
It is clear that since the argument $\omega_n(t)$, (8b), of the sinsoidal functions in (10) is not linear in (t) due to the beating frequency term, $\frac{\sin(2n\tau)}{2n}$, the periodic sine and cosine patterns are shown for large interval of τ. The effect of the beating frequency is shown in the zooming insets in Fig.(2a,b) as very weak oscillations in the main envelopes of the sine and cosine functions. For $n \gg 1$, the beating frequency term tends to vanish, and hence the main periodic patterns occur over much shorter time interval τ and have no (beating) oscillations as in the zooming insets.

(ii) *Initial atomic coherent state* $|\theta, \phi\rangle$

In this case the atom initially in the state,

$$|\theta, \phi\rangle = \cos(\frac{\theta}{2})|g\rangle + \sin(\frac{\theta}{2})e^{-i\phi}|e\rangle \tag{11}$$

with $\theta \in [0, \pi]$ and $\phi \in [0, 2\pi]$ are the excitation and phase parameters (cf.[23, 24]). In this case [19],

$$\langle\hat{\sigma}_{\pm}(0)\rangle_{\theta,\phi} = \frac{1}{2}\sin(\theta)e^{i\pm\phi}$$
$$\langle\hat{\sigma}_z(0)\rangle_{\theta,\phi} = -\frac{1}{2}\cos(\theta) \tag{12}$$

and hence the time-dependent atomic averages of (6) have the forms,

$$\langle\hat{\sigma}_{+}(\tau)\rangle_{\theta,\phi} = \frac{1}{2}\sin\theta\cos\phi + \frac{i}{2}\left(\cos\theta\sin(\omega_n(\tau)) + \sin\theta\sin\phi\cos(\omega_n(\tau))\right)$$

$$\langle\hat{\sigma}_z(\tau)\rangle_{\theta,\phi} = -\frac{1}{2}\cos\theta\cos(\omega_n(\tau)) + \frac{1}{2}\sin\theta\sin\phi\sin(\omega_n(\tau)). \tag{13}$$

Note, in this case the time-independent dispersive atomic polarisation component is non-zero, $Re\langle\sigma_+(\tau)\rangle_{\theta,\phi} = \frac{1}{2}\sin\theta\cos\phi$, due to the non-zero initial dispersion,
$0 < \theta < \pi$. The effect of the initial coherent state parameters (θ, ϕ), as compared with the initial ground state $(\theta = 0)$ is shown in Fig.(2a,b) where we notice that same periodic behaviour but with lesser (larger) maximum (minimum) values.

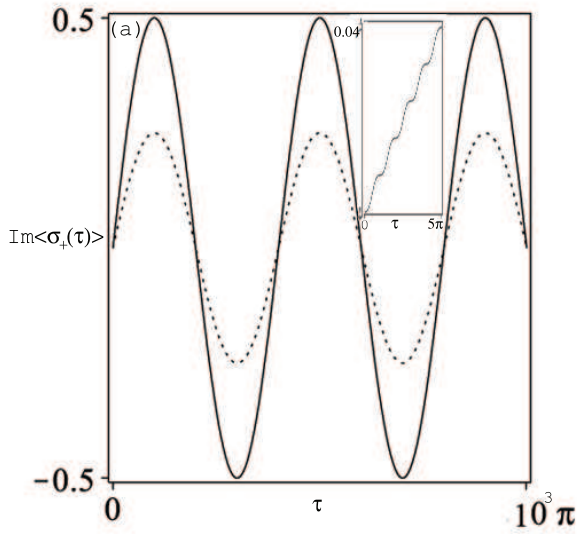

Fig.2a: Plot of $Im\langle\hat{\sigma}_+(\tau)\rangle$ for both cases of initial ground state (full lines) and initial coherent state $(\theta = \frac{\pi}{3}, \phi = 0)$ (dotted lines) with, $n = 1, \Omega' = 0.01$. Inset shows the zooming of the beating frequency in the interval $[0, 5\pi]$

3. The Transient Spectrum

The formula for the transient spectrum is given by [25],

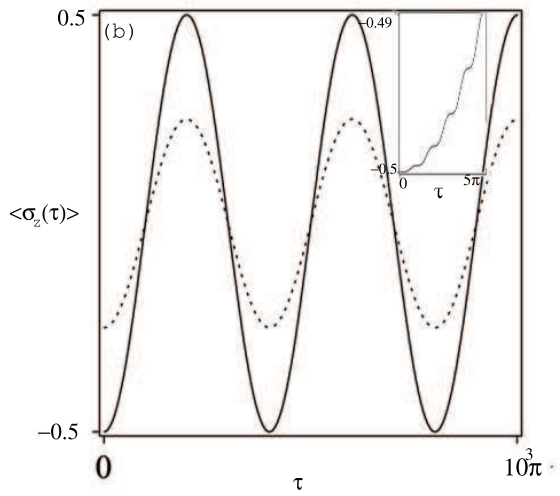

Fig.2b: As Fig.2a but for the atomic inversion $\langle\hat{\sigma}_z(\tau)\rangle$.

,

$$S(t,D,\Gamma) = 2\Gamma \int_0^t dt_1 \int_0^t dt_2 e^{(-\Gamma+i\omega_f)(t-t_1)} \times e^{(-\Gamma-i\omega_f)(t-t_2)} \langle \hat{S}_+(t_1)\hat{S}_-(t_2)\rangle \tag{14}$$

where, $\langle \hat{S}_+(t_1)\hat{S}_-(t_2)\rangle$ is the auto-correlation function for the atomic dipole operators, ω_f and Γ are the frequency and width of the detector's filter, respectively. The auto-correlation function for arbitrary initial atomic state is given by [19]

$$\begin{aligned}\langle \hat{S}_+(t_1)\hat{S}_-(t_2)\rangle &= e^{i\omega_l(t_1-t_2)}\langle \hat{\sigma}_+(t_1)\hat{\sigma}_-(t_2)\rangle \\ &= e^{i\omega_l(t_1-t_2)}\langle [C_+(t_1)\hat{\sigma}_+(0) + C_-(t_1)\hat{\sigma}_-(0) + C_z(t_1)\hat{\sigma}_z(0)] \\ &\times \left[C_+^*(t_2)\hat{\sigma}_-(0) + C_-^*(t_2)\hat{\sigma}_+(0) + C_z^*(t_2)\hat{\sigma}_z(0)\right]\rangle \end{aligned} \tag{15}$$

We consider the following two cases of initial atomic state.

3.1. Initial Ground State

If the atom is initially in the ground state $|g\rangle$ then the use of (9) into (15) gives,

$$\langle \hat{S}_+(t_1)\hat{S}_-(t_2)\rangle_g = e^{i\omega_1(t_1-t_2)}\left(A_-(t_1)A_-^*(t_2)+\frac{1}{4}A_z(t_1)A_z^*(t_2)\right) \tag{16}$$

Using (16) into (14), we get,

$$\begin{aligned} S_g(t,D,\Gamma) &= 2\Gamma e^{-2\Gamma t}\int_0^t dt_1\int_0^t dt_2 e^{(-\Gamma+iD)t_2+(-\Gamma-iD)t_1} \\ &\quad\times\left(C_-(t_1)C_-^*(t_2)+\frac{1}{4}C_z(t_1)C_z^*(t_2)\right) \\ &= 2\Gamma e^{-2\Gamma t}\left(|\, I_1(t)|^2+|\, I_2(t)|^2\right) \end{aligned} \tag{17}$$

where $D=\omega_f-\omega_o$ is the detector's detuning parameters and the expressions $I_{1,2}(t)$ are given as follows,

$$\begin{aligned} I_1(t) &= \int_0^t e^{(\Gamma+iD)t_1}C_-(t_1)dt_1 \\ &= \frac{1}{2}\int_0^t e^{(\Gamma+iD)t_1}(1-cos\,\omega(t_1))dt_1 \\ &= \frac{e^{(\Gamma+iD)t}-1}{2(\Gamma+iD)}-\frac{1}{4}(A_k(\Omega)+A_k(\Omega\to-\Omega)), \end{aligned} \tag{18a}$$

$$\begin{aligned} I_2(t) &= \frac{1}{2}\int_0^t e^{(\Gamma+iD)t_1}C_z(t_1)dt_1 \\ &= -\frac{i}{2}\int_0^t e^{(\Gamma+iD)t_1}sin\,\omega(t_1)dt_1 \\ &= -\frac{1}{4}(F_k(\Omega)+F_k(\Omega\to-\Omega)) \end{aligned} \tag{18b}$$

with,

$$A_k(\Omega)=\sum_{k=0}^{\infty}J_k(\frac{\Omega}{4n\omega_o})\left(\frac{e^{(\Gamma+i(D+\frac{\Omega}{2}-2kn\omega_o))t}-1}{(\Gamma+i(D+\frac{\Omega}{2}-2kn\omega_o))}+\frac{e^{(\Gamma+i(D-\frac{\Omega}{2}+2kn\omega_o))t}-1}{(\Gamma+i(D-\frac{\Omega}{2}+2kn\omega_o))}\right) \tag{19a}$$

$$F_k(\Omega)=\sum_{k=0}^{\infty}J_k(\frac{\Omega}{4n\omega_o})\left(\frac{e^{(\Gamma+i(D+\frac{\Omega}{2}-2kn\omega_o))t}-1}{(\Gamma+i(D+\frac{\Omega}{2}-2kn\omega_o))}-\frac{e^{(\Gamma+i(D-\frac{\Omega}{2}+2kn\omega_o))t}-1}{(\Gamma+i(D-\frac{\Omega}{2}+2kn\omega_o))}\right) \tag{19b}$$

and $J_k(\frac{\Omega}{4n\omega_0})$ is the Bessel function of order (k).
In general the expressions for the spectrum, (17)-(19) is composed of the Mollow triplet [1] with terms for $k = 0$, while the terms for $(k, n) \neq 0$ contain the whole harmonics of the spectrum due to the n-sequential laser pulses, with oscillatory weights associated with Bessel functions $J_k(\frac{\Omega}{4n\omega_0})$ of order k and argument dependent on the pulse strength (Ω) and pulse number (n).
The scaled spectrum $S_g(D') = \dfrac{S_g(t, D', \Gamma)}{\max(S_g(t, D', \Gamma))}$ is plotted in Fig.3 against $D' = \frac{D}{\Gamma}$ for fixed width $\Gamma' = \frac{\Gamma}{\omega_0} = 0.05$ and $n = 1$. For fixed $\tau = 10\pi$ (so, 10 exciting pulses each of π-duration over the period $[0, 10\pi]$) and increasing pulse strength Ω'', $(\Omega'' = \frac{\Omega}{\Gamma})$ (Fig.3a) the spectrum has a single Lorentzian peak surrounded by weak oscillations for weak $\Omega'' = 0.5$ which develops with stronger $\Omega'' = 50$ to three-Lorentzian peak structure with inter-ringing (chain of oscillations) due to the multi-pulse excitation.
For fixed pulse strength $\Omega'' = 10$ and increasing time detection τ (Fig.3b), the spectrum develops from a broad central Lorentzian with surrounded weak oscillations to a splitting in the central Lorentzian (hole burning) with relatively pronounced oscillations and eventually to a narrowed Lorentzian with larger $\tau = 5\pi$ with vanishing oscillations. This shows that the 3-peak structure with oscillations occur with much larger values of $\Omega'' = 50, \tau = 10\pi$ (i.e. larger number of pulses), while the hole burning structure with pronounced oscillations occur with strong $\Omega'' = 10$ but washes away with increasing time $\tau = 5\pi$. For lesser $\Omega'' = 5$ the same occurs, but with hole burning dip structure washes away with larger $\tau > 5\pi$.

3.2. Initial Coherent State

If the atom starts in the coherent state $|\theta, \phi\rangle$, (11), then the use of the initial mean values in (12) into (15) then gives [19],

$$\begin{aligned}\langle \hat{S}_+(t_1)\hat{S}_-(t_2)\rangle = e^{i\omega_l(t_1-t_2)} \\ [\cos^2\frac{\theta}{2}C_-(t_1)C_-^*(t_2) + \sin^2\frac{\theta}{2}C_+(t_1)C_+^*(t_2) \\ + \frac{1}{4}C_z(t_1)C_z^*(t_2) + \frac{1}{4}C_-(t_1)C_z^*(t_2) - \frac{1}{4}C_z(t_1)C_+^*(t_2) \\ \times \sin\theta e^{i\phi} - \frac{1}{4}C_+(t_1)C_z^*(t_2) - \frac{1}{4}C_z(t_1)C_-^*(t_2) \\ \times \sin\theta e^{i\phi}]. \qquad (20)\end{aligned}$$

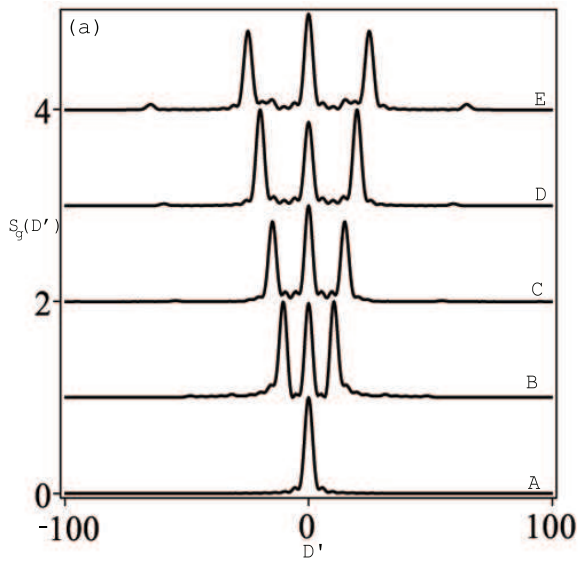

Fig.3(a): The spectrum $S_g(D')$ against the normalised detector's detuning parameter D' for $\tau = 10\pi, n = 1, \Gamma' = 0.05$ and increasing pulse strength Ω''. The curves $A[S](\Omega'' = 0.5)$, $B[S+1](\Omega'' = 20)$, $C[S+2](\Omega'' = 30)$, $D[S+3](\Omega'' = 40)$ and $E[S+4](\Omega'' = 50)$

Using (20) into (14) we finally get,

$$S(t,D,\Gamma)_{\theta,\phi} = 2\Gamma e^{-2\Gamma t}[\mid I_1(t)\mid^2 cos^2(\frac{\theta}{2}) + \mid I_2(t)\mid^2 + \mid I_3(t)\mid^2 sin^2(\frac{\theta}{2}) - \frac{1}{2}Re(I_3(t)I_4(t)\sin\theta e^{i\phi}) + \frac{1}{2}Re(I_1(t)I_4(t)\sin\theta e^{-i\phi})] \quad (21)$$

where,

$$\begin{aligned} I_3(t) &= \int_0^t e^{(\Gamma+iD)t_1} C_+(t_1)dt_1 \\ &= \frac{1}{2}\int_0^t e^{(\Gamma+iD)t_1}(1+cos\,\omega(t_1))dt_1 \\ &= \frac{e^{(\Gamma+iD)t}-1}{2(\Gamma+iD)} + \frac{1}{4}(A_k(\Omega) + A_k(\Omega\to-\Omega)), \quad (22a) \\ I_4(t) &= \int_0^t e^{(\Gamma+iD)t_1} C_z^*(t_1)dt_1 \end{aligned}$$

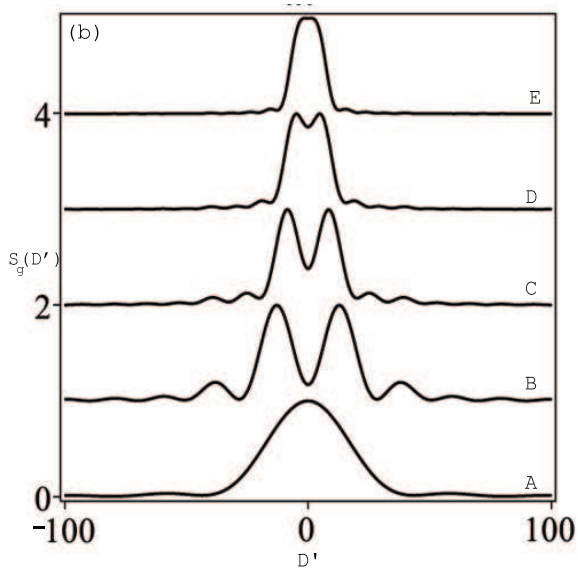

Fig.3(b): As Fig.3a but for $\Omega'' = 10$ and increasing detection time τ. The curves $A[S](\tau = \pi)$, $B[S+1](\tau = 2\pi)$, $C[S+2](\tau = 3\pi)$, $D[S+3](\tau = 4\pi)$ and $E[S+4](\tau = 5\pi)$.

$$= i \int_0^t e^{(\Gamma + iD)t_1} sin\, \omega(t_1) dt_1$$
$$= -2I_2(t). \tag{22b}$$

The form $S_{\theta,\phi}(t, D, \Gamma)$ in (21) compared the initial ground state case, $S_g(t, D, \Gamma)$ in (17), has essentially two additional terms: the 3rd term in $|I_3(t)|^2$ is proportional to the spectrum of the excited state and the last term represents an interference between amplitude spectra of atomic inversion and atomic polarisation in the presence of the initial dipole component $\langle \hat{\sigma}_{\pm}(0) \rangle = \frac{1}{2} \sin\theta e^{i\pm\phi}, 0 < \theta < \pi$ [19].

The plot of the scaled spectrum $S_{\theta,\phi}(D') = \dfrac{S_{\theta,\phi}(t, D', \Gamma)}{\max S_{\theta,\phi}(t, D', \Gamma)}$ is presented in Fig.4a for fixed strong $\Omega'' = 40$ and $(\theta = \frac{\pi}{3}, \phi = 0)$. The spectrum has a pronounced asymmetry: It has a single broad peak at small $\tau = \pi$ (single pulse) with tendency of splittings and then develops to a clear 3-peak structure with (weak) ringing phenomena due to the interference of the multiple pulse with strong Rabi oscillations for larger $\tau = 5\pi$(five pulses). So the ringing is enhanced with the non-zero initial atomic dipoles $\langle \sigma_{\pm}(0) \rangle = \frac{1}{2} \sin\theta e^{\pm i\phi}, 0 < \theta <$

π. This is qualitatively similar to the rectangular pulse case [19].

The increase of the detection time $\tau = 10\pi \rightarrow 50\pi$ has different effects on the spectrum $S_{\theta,\phi}(D')$, depending on the coherent parameters and the pulse strength Ω''. In Fig.(4b), for $\Omega'' = 5$ and $(\theta = \frac{\pi}{4}, \phi = \pi)$ the broad Lorentzian at $\tau = 10\pi$ has tendency to split to 3-peaks at its peak, but eventually shows a hole burning dip structure with larger $\tau = 50\pi$ with no oscillations. For different $\Omega'' = 10$ and $(\theta = \phi = \frac{\pi}{4})$, Fig.4c, the splitted Lorentzian at its peak develops to 3-peak structure with no oscillations.

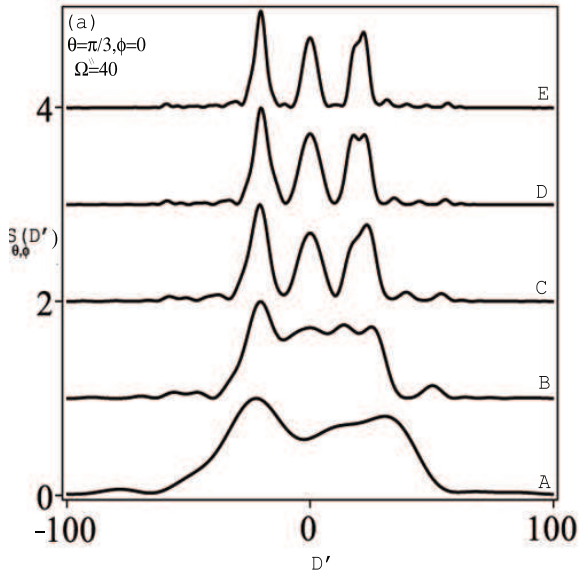

Fig.4(a): The spectrum $S_{\theta,\phi}(D')$ for $n = 1, \Gamma' = 0.05, \Omega'' = 40$ and $(\theta = \frac{\pi}{3}, \phi = 0)$ and inceasing τ. The curves $A[S](\tau = \pi)$, $B[S+1](\tau = 2\pi)$, $C[S+2](\tau = 3\pi)$, $D[S+3](\tau = 4\pi)$ and $E[S+4](\tau = 5\pi)$.

4. Summary

The model of a pulsed-driven 2-level atom is investigated in case of a resonant $\sin^2$-pulse shape and in the absence of any dissipative processes. The explicit exact solution for the atomic variables are used to calculate the transient scattered spectrum for arbitrary system parameters. The main results are:

(i) The mean atomic polarisation and inversion have their sinusoidal periodic

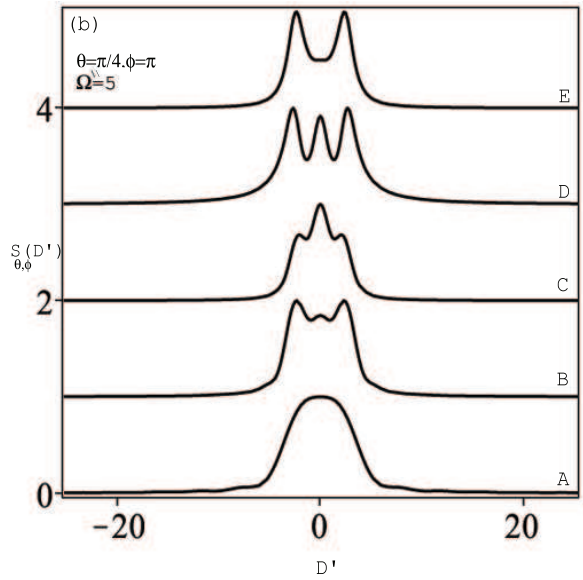

Fig.4(b): As Fig.4a but with $\Omega'' = 5, \theta = \frac{\pi}{4}, \phi = \pi$ and increasing detection time τ. The curves $A[S](\tau = 10\pi)$, $B[S+1](\tau = 20\pi)$, $C[S+2](\tau = 30\pi)$, $D[S+3](\tau = 40\pi)$ and $E[S+4](\tau = 50\pi)$.

envelope with beating frequency due to the multiple-sequntial pulses at the $\sin^2$-pulse.

(ii) For strong pulse strength (Rabi frequency) the main 3-Lorentzian structure of the transient spectrum exhibits pronounced asymmetry with ringing (chain of oscillations) due to initial atomic coherence.

The ringing is essentially due to the interference of the many sequential-pulse with the non-zero initial dispersive atomic coherent dipole component. For relatively smaller pulse strength, the main Lorentzian peak shows 'hole burning' effect (i.e. reduction of emitted resonant radiation) with no ringing effect.
Finally, we may add that detection of such weak 'ringing' radiation, which is desirable in signal information processing [26, 27], is possible in the light of experimental detection of ultra weak signals [28] and fields [29].

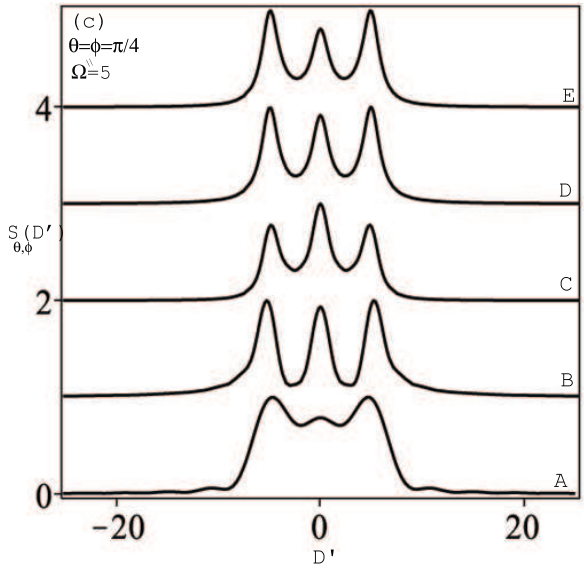

Fig.4(c): As Fig.4a but with $\Omega'' = 5, \theta = \phi = \frac{\pi}{4}$ and increasing detection time τ. The curves $A[S](\tau = 10\pi)$, $B[S+1](\tau = 20\pi)$, $C[S+2](\tau = 30\pi)$, $D[S+3](\tau = 40\pi)$ and $E[S+4](\tau = 50\pi)$.

Acknowledgments

The author acknowledges gratitude to King Abdul Aziz University, Deanship of Scientific Research (Jeddah, KSA) for the financial support of this work (project number 247-500). The author also acknowledges fruitful discussions with Prof. Shoukry S. Hassan(University of Bahrain).

References

[1] B.R. Mollow, Power spectrum of light scattered by two-level system, *Phys. Rev.*, **188**, **doi: http://dx.doi.org/10.1103/** (1969), 1969-1975.

[2] F. Schuda, C. R. Stroud Jr. and M. Herscher, Observation of the resonant Stark effect at optical frequencies, *J. Phys. B*, **7**, **doi:10.1088/0022-3700/7/7/002** (1974), L198-L202.

[3] F. Y. Wu, R. E. Grove and S. Ezekiel, Investigation of the Spectrum of

Resonance Fluorescence Induced by a Monochromatic Field, *Phys. Rev. Lett.*, **35**, **doi: 10.1103/** (1975)1426-1429.

[4] W. Hartig, W. Rasmussen, R. Schneider and H. Walther, Study of the frequency distribution of the fluorescent light induced by monochromatic radiation, *Z. Phys. A*, **278**, **doi:10.1007/BF01409169** (1976), 205-210.

[5] B. W. Shore, The Theory of Coherent Atomic Excitation, (Wiley, New York, 1990).

[6] P. Gibbon, Short Pulse Laser Interactions with Matter, (Imperial College Press, London, 2005).

[7] A. Ekert and R. Jozsa, Quantum computation and Shor's factoring algorithm, *Rev. Mod. Phys.*, **68**, **doi: http://dx.doi.org/10.1103/RevModPhys.68.733** (1996)733-753.

[8] P. Zoller et al., Quantum information processing and communication, *Eur. Phys. J.D*, **36**, **doi: 10.1140/epjd/e2005-00251-1** (2005), 203-228.

[9] A. Khare, K. Alti, S. Das, A. S. Patra, M. Sharma, Application of laser matter interaction for generation of small-sized materials, *Radiation Physics and Chemistry*, **70**, **doi: 10.1016/j.radphyschem.2003.12.038** (2004), 553-558.

[10] Y.-X. Yan, E. B. Gamble, and K. A. Nelson, Impulsive stimulated scattering: General importance in femtosecond laser pulse interactions with matter, and spectroscopic applications, *J. Chem. Phys.*, **83**, **doi: 10.1063/1.449708** (1985), 5391-5399.

[11] D. Felinto, C.A.C. Bosco, L.H. Acioli, S.S. Vianna, Coherent accumulation in two-level atoms excited by a train of ultrashort pulses, *Opt. Commun.* **215**, **doi: 10.1016/S0030-4018(02)02230-7** (2003), 69-73.

[12] T. Rickes, L.P. Yatsenko, S. Steuerwald, T. Halfmann, B. W. Shore, N.V. Vitanov, and K. Bergmann, Efficient adiabatic population transfer by two-photon excitation assisted by a laser-induced Stark shift, *J. Chem. Phys.*, **113**, **doi:http://dx.doi.org/10.1063/1.481829** (2000), 534-546.

[13] Y.A. Sharaby, A. Joshi, and S. S. Hassan, Coherent Population Transfer in V-Type Atomic System, *J. Nonlinear Optic. Phys.& Materials.*, **22**, **doi: 10.1142/S0218863513500446** (2013), 1350044-59.

[14] K. Rzazewski and M. Florjanczyk, The resonance fluorescence of a two-level system driven by a smooth pulse, *J. Phys. B: At. Mol. Phys.*, **17**, **doi:10.1088/0022-3700/17/15/005** (1984), L509-L513.

[15] M. Lewenstein, J. Zakrzewski, K. Rzazewski, Theory of fluorescence spectra induced by short laser pulses, *J. Opt. Soc. Am. B*, **3**, **doi:http://dx.doi.org/10.1364/JOSAB.3.000022** (1986), 22-35.

[16] J. Zakrzewski, M. Lewenstein and R. Kuklinski, Soluble models of optical systems driven by exponential pulses, *J. Phys. B*, **18**, **10.1088/0022-3700/18/23/014** (1985), 4631-4637.

[17] P.A. Rodgers and S. Swain, Multi-peaked resonance fluorescence spectra with rectangular laser pulses, *Opt. Commun.*, **81**, **doi: 10.1016/0030-4018(91)90618-N** (1991), 291-296.

[18] A Joshi and S S Hassan, Resonance fluorescence spectra of a two-level atom and of a harmonic oscillator with multimode rectangular laser pulses, *J. Phys. B*, **35**, **doi:10.1088/0953-4075/35/9/301** (2002), 1985-2003.

[19] S.S. Hassan, A. Joshi, N.M.M. Al-Madhari, Spectrum of a pulsed driven qubit, *J. Phys.B*, **41**, **doi:10.1088/0953-4075/41/14/145503** (2008)145503-09; (Corrigendum), **42**, **doi:10.1088/0953-4075** (2009), 089801.

[20] S.S. Hassan, A. Joshi and H.A. Batarfi, Spectrum of a triangular pulsed-driven atom, *Int. J. Theoret. Phys. Group Theory and Nonlinear optics (Nova Sci. Pub.)*, **13**, **3/4** (2010), 371-382.

[21] H.A. Batarfi, Spectrum of spin$-\frac{1}{2}$ system driven by resonant exponential pulse,*J. Nonlinear Optic. Phys.& Materials.*, **21**, **doi: 10.1142/S0218863512500257** (2012), 1250025-49.

[22] S.S. Hassan, M.A. AL-Saegh, A. S. Mohamed and H.A. Batarfi, Haar Wavelet Spectrum of a Pulsed-Driven Qubit, *Nonlinear Optics and Quantum Optics*, **42**, **doi:1543-0537** (2011), 37-50.

[23] J.M. Radcliffe, Some properties of coherent spin states, *J. Phys. A: Gen. Phys.*, **4**, **doi:10.1088/0305-4470/4/3/009** (1971), 313-323.

[24] F.T. Arrechi, E. Coutness, R. Gilmore and H. Thomas, Atomic coherent states in quantum optics, *Phys. Rev. A*, **6**, **doi:http://dx.doi.org/10.1103/PhysRevA.6.2211** (1972), 2211-2237.

[25] J.H. Eberly, K. Wodkiewicz, The time-dependent physical spectrum of light, *J. Opt. Soc.Am*, **67**, **doi:.org/10.1364/JOSA.67.001252** (1977), 1252-1261.

[26] M.F. Yanik, S. Fan and M. Soljacic, High-contrast all-optical bistable switching in photonic crystal microcavities, *Appl. Phys. Lett.*, **83**, **doi:http://dx.doi.org/10.1063/1.1615835** (2003), 2739-2741.

[27] H. Mabuchi, Coherent-feedback control strategy to suppress spontaneous switching in ultralow power optical bistability, *App. Phys. Lett.*, **98**, **doi:http://dx.doi.org/10.1063/1.3589994** (2011), 193109-3.

[28] http://www.ornl.gov/sci/engineering-science-technology sms/Hardy %20Fact %20Sheets/Ultra-Weak %20Signal.pdf.

[29] D.F. Walls, Squeezed states of light, *Nature*, **306**, **10.1038/306141a0** (1983), 141-146.